The 2-Silaketenylidene (CSiO) Radical: Electronic Structure of the $\tilde{X}\ ^3\Sigma^-$ and $\tilde{A}\ ^3\Pi$ States†

Nicholas D. K. Petraco, Shawn T. Brown, Yukio Yamaguchi, and Henry F. Schaefer III*

Center for Computational Quantum Chemistry, University of Georgia, Athens, Georgia 30602

Received: March 22, 2000; In Final Form: May 18, 2000

A theoretical study, using ab initio electronic structure theory, of the ground ($\tilde{X}\ ^3\Sigma^-$) and first excited triplet ($\tilde{A}\ ^3\Pi$) electronic states of the 2-silaketenylidene (CSiO) radical has been reported. The $\tilde{A}\ ^3\Pi$ state is subject to a Renner−Teller interaction and possesses two distinct real vibrational frequencies along the bending coordinate. To avoid variational collapse to a lower-lying state, the $^3A''$ component of the $\tilde{A}\ ^3\Pi$ state was investigated using the equation of motion (EOM) CCSD technique. With the TZ3P(2f) EOM-CCSD method, the Renner parameter (ϵ) and bending harmonic vibrational frequency (ω_2) for the $\tilde{A}\ ^3\Pi$ state were determined to be $\epsilon = -0.253$ and $\omega_2 = 337$ cm^{-1}. At the highest level of theory, cc-pVQZ CCSD(T), the classical $\tilde{X}-\tilde{A}$ splitting of CSiO was predicted to be 29.8 kcal/mol (1.29 eV, 10 400 cm^{-1}), and the quantum mechanical energy separation to be 31.1 kcal/mol (1.35 eV, 10 900 cm^{-1}). The ground state of CSiO lies 65.4 kcal/mol above the ground state of SiCO. The bond energy for C−SiO was determined to be $D_e = 32.6$ ($D_0 = 31.4$) kcal/mol, indicating considerable stability for the ground state of CSiO against the dissociation reaction CSiO ($\tilde{X}\ ^3\Sigma^-$) → C (^{3}P) + SiO ($\tilde{X}\ ^1\Sigma^+$). The most remarkable prediction from the present research is that the C−Si distance in the $\tilde{A}\ ^3\Pi$ excited state is nearly 0.2 Å less than that in the $\tilde{X}\ ^3\Sigma^-$ ground state. In fact, this distance (1.662 Å) is one of the shortest known Si−C bond distances with a formal bond order of $^5/_2$.

I. Introduction

The ketenylidene radical (CCO) is known to be an important reactive intermediate involved in many chemical reactions in the gas phase.[1] This molecule has also been detected in the cold, dark interstellar molecular cloud TMC-1 by microwave spectroscopy.[2] The first spectroscopic study of the free radical CCO using the matrix-isolated infrared (IR) technique was performed by Jacox et al. in 1965.[3] They detected the three vibrational fundamentals of CCO in an argon matrix at 381, 1074, and 1978 cm^{-1}. The absorption spectrum in the region 5000−6500 Å was observed by Devillers during the flash photolysis of carbon suboxide and was tentatively attributed to the CCO molecule.[4] These observations were extended to 9000 Å by Devillers and Ramsay.[5] The strong band near 8580 Å (11 650 cm^{-1}) was assigned as the 000−000 band of the $\tilde{A}\ ^3\Pi \leftarrow \tilde{X}\ ^3\Sigma^-$ transition.[5] In 1977, Lembke et al. reported electron spin resonance (ESR) and optical spectra of the SiCO, SiN_2, and $Si(CO)_2$ molecules.[6] From the ultraviolet absorption spectrum in an argon matrix at 4 K, they determined the $\tilde{X}-\tilde{A}$ splitting of SiCO, an isovalent isomer of CCO, to be 24 056 cm^{-1}.[6] For other experimental studies on the CCO and SiCO radicals, readers should refer to the superb compilation by Jacox.[7]

The ground and first excited triplet electronic states of the isovalent species, CCO and SiCO, are experimentally[1−7] and theoretically[8−17] determined to be $\tilde{X}\ ^3\Sigma^-$ and $\tilde{A}\ ^3\Pi$ states, respectively, and they both present linear structures. The $\tilde{A}\ ^3\Pi$ states of CCO and SiCO are subjected to Renner−Teller interactions[18−25] and have two distinct vibrational frequencies along the bending coordinates. In two recent papers we have reported systematic studies for the ground and first excited triplet states of CCO[15] and SiCO[17] in their linear forms. For these two ketenylidene radicals, it was demonstrated that the theoretical relative energies of the $\tilde{X}$ and $\tilde{A}$ states are converging in the direction of the experimental values in terms of basis set expansion and correlation level. At the highest level of theory employed, cc-pVQZ CCSD(T), the theoretically predicted $\tilde{X}-\tilde{A}$ splittings for the CCO and SiCO molecules agreed with the experimental values within a chemical accuracy of ±1 kcal mol. The present study for the CSiO molecule is a logical extension of our previous studies. To the best of our knowledge there are no experimental or theoretical investigations on the CSiO molecule. The two lowest-lying triplet states of CSiO will be investigated employing the self-consistent-field (SCF), configuration interaction with single and double excitations (CISD), coupled-cluster with single and double excitations (CCSD), and CCSD with perturbative triple excitations [CCSD(T)] methods with a wide range of basis sets. For the first excited triplet state ($\tilde{A}\ ^3\Pi$), the equation-of-motion (EOM) CCSD technique is also utilized to overcome possible variational collapse to a lower-lying state. The results for the CSiO molecule will be compared with those for the CCO and SiCO species.

II. Electronic Structure Considerations

The electronic ground state of the linear CSiO radical has the electronic configuration

$$[\text{core}](6\sigma)^2(7\sigma)^2(8\sigma)^2(2\pi)^4(9\sigma)^2(3\pi_i)(3\pi_o) \qquad \tilde{X}\ ^3\Sigma^- \quad (1)$$

where [core] denotes the seven core (for Si, 1s-, 2s-, and 2p-like and for C and O, 1s-like) orbitals and π_i and π_o stand for in-plane and out-of-plane π orbitals, respectively. The 6σ and 7σ molecular orbitals (MOs) mainly represent the Si−O and C−Si σ bonds, whereas the 8σ and 9σ MOs are the lone-pair orbitals on the O and C atoms. The 2π and 3π MOs are attributed to the Si−O and C−Si π bonds, respectively. The 9σ and 3π MOs for the ground state of CSiO are depicted in

† Part of the special issue "C. Bradley Moore Festschrift".

* Author to whom correspondence should be addressed. Fax: +1 706-542-0406.

10.1021/jp001080w CCC: $19.00 © 2000 American Chemical Society
Published on Web 07/11/2000

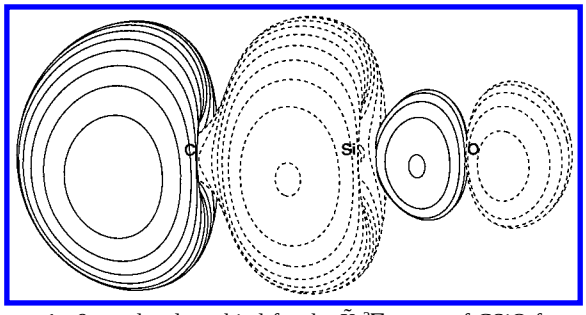

Figure 1. 9σ molecular orbital for the $\tilde{X}\ ^3\Sigma^-$ state of CSiO from the TZ2P(f) SCF method.

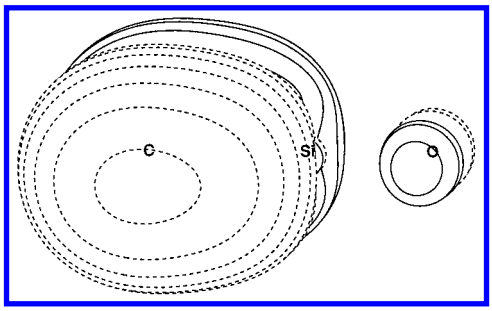

Figure 2. $3\pi_o$ molecular orbital for the $\tilde{X}\ ^3\Sigma^-$ state of CSiO from the TZ2P(f) SCF method.

Figures 1 and 2, respectively. Upon bending, the molecular symmetry for the $^3\Sigma^-$ ground state of CSiO reduces to a $^3A''$ state, producing a real degenerate bending vibrational frequency. The first excited triplet state of CSiO is a single-electron excitation

$$(9\sigma)^2(3\pi)^2 \rightarrow (9\sigma)(3\pi)^3 \tag{2}$$

to the electronic configuration

$$[\text{core}](6\sigma)^2(7\sigma)^2(8\sigma)^2(2\pi)^4(9\sigma)(3\pi)^3 \qquad \tilde{A}\ ^3\Pi \tag{3}$$

Upon the bending motion, the $\tilde{A}\ ^3\Pi$ state splits into $^3A'$ and $^3A''$ states. Thus, this $\tilde{A}\ ^3\Pi$ state presents the two distinct real vibrational frequencies along the bending coordinates. In other words, the $\tilde{A}\ ^3\Pi$ state of CSiO is subjected to Renner−Teller interaction,[18−25] and it is a type A Renner−Teller molecule, as classified by Lee et al., for linear triatomic molecules.[24]

It may be appropriate to discuss the molecular orbital Hessian[26] of the reference self-consistent-field wave functions in this section. At the linear configuration, the MO Hessian for the $\tilde{X}\ ^3\Sigma^-$ state of CSiO shows all positive eigenvalues, as expected. Thus, the SCF wave function for the $\tilde{X}\ ^3\Sigma^-$ state of CSiO is *stable*. The $\tilde{A}\ ^3\Pi$ state of CSiO has one zero and one negative eigenvalues of the MO Hessian. The eigenvector of the negative eigenvalue is associated with the $9\sigma-3\pi$ MO rotation. Thus, the SCF wave function for the $\tilde{A}\ ^3\Pi$ state of CSiO is *unstable*, and a lower-lying state at the $\tilde{A}\ ^3\Pi$ equilibrium geometry exists. The magnitudes for the eigenvalues of the MO Hessian may also provide useful information for the stability of the SCF reference wave function.[26−28]

During the two stretching vibrational motions, the spatial symmetries for the $\tilde{X}\ ^3\Sigma^-$ and $\tilde{A}\ ^3\Pi$ states of CSiO remain the same. Consequently, these two stretching vibrational frequencies of the two triplet states can be determined without the variational collapse of the reference (SCF) wave functions. The bending vibrational frequencies of the $\tilde{X}\ ^3\Sigma^-$ state and the $^3A'$ component of the $\tilde{A}\ ^3\Pi$ state can be also obtained correctly because of the spatial orthogonality of the reference SCF wave functions. However, the $^3A''$ component of the $\tilde{A}\ ^3\Pi$ state is the second state of its symmetry. Because the typical one-configuration SCF wave function can not be used for the $^3A''$ component of the $\tilde{A}\ ^3\Pi$ state, the EOM-CCSD technique was utilized, and the $^3A''$ component was obtained as the second root ($2\ ^3A''$) of the reference bent ground state ($1\ ^3A''$).

III. Renner−Teller Interaction

As mentioned above, the $\tilde{A}\ ^3\Pi$ state of CSiO is subjected to Renner−Teller interaction[18−25] and presents two distinct bending vibrational frequencies. Following the discussion by Herzberg,[21] the Renner parameter (ϵ), which is a measure of the strength of the vibronic interaction, can be described in the following manner. The average potential (V^0) of the "upper" (V^+) and "lower" (V^-) bending modes can be given, neglecting the anharmonic terms, as

$$V^0 = \frac{V^+ + V^-}{2} = ar^2 \tag{4}$$

and the splitting into V^+ and V^- produced by the vibronic interaction can be represented by a similar equation

$$V = V^+ - V^- = \alpha r^2 \tag{5}$$

where r is the bending coordinate and a and α are the force constants. The terms upper and lower are arbitrary in this section and are used to distinguish the two distinct bending motions. The Renner parameter (ϵ) is defined by

$$\epsilon = \frac{V^+ - V^-}{V^+ + V^-} = \frac{\alpha}{2a} \tag{6}$$

It can be shown that eq 6 is equivalent to

$$\epsilon = \frac{f^+ - f^-}{f^+ + f^-} = \frac{(\omega^+)^2 - (\omega^-)^2}{(\omega^+)^2 + (\omega^-)^2} \tag{7}$$

where f^+ and f^- and ω^+ and ω^- are the force constants and harmonic frequencies associated with the upper and lower bending potentials, respectively. Denoting μ to be the kinetic energy contribution to the bending motion, the harmonic bending frequency (ω_2) can be determined using the equation

$$\omega_2 = \frac{1}{2\pi c}\sqrt{\frac{a}{\mu}} = \frac{1}{2\pi c}\sqrt{\frac{f^+ + f^-}{2\mu}} \tag{8}$$

which can be rewritten as

$$\omega_2 = \sqrt{\frac{1}{2}[(\omega^+)^2 + (\omega^-)^2]} \tag{9}$$

Finally, the upper and lower bending frequencies are related to the ω_2 frequency using the Renner parameter by

$$\omega^{\pm} = \omega_2\sqrt{1 \pm \epsilon} \tag{10}$$

Utilizing eqs 4−10, the experimentally observable values, ϵ and ω_2, can be compared with the corresponding theoretical values that can be evaluated completely independently.

IV. Theoretical Procedures

Eight basis sets were employed in order to determine structures and physical properties. The basis sets of triple-ζ (TZ) quality for C and O are obtained from Dunning's triple-ζ

TABLE 1: Optimized Structures for the $\tilde{X}\ ^3\Sigma^-$ and $\tilde{A}\ ^3\Pi$ States of the CSiO Molecule[a]

electronic state	$\tilde{X}\ ^3\Sigma^-$ state		$\tilde{A}\ ^3\Pi$ state	
level of theory	r_e(CSi)	r_e(SiO)	r_e(CSi)	r_e(SiO)
TZ2P SCF	1.8291	1.4760	1.6266	1.4823
TZ2P+diff SCF	1.8290	1.4763	1.6269	1.4825
TZ3P SCF	1.8270	1.4738	1.6240	1.4795
TZ2P(f) SCF	1.8273	1.4756	1.6255	1.4818
TZ2P(f)+diff SCF	1.8272	1.4760	1.6257	1.4822
TZ3P(2f) SCF	1.8248	1.4723	1.6243	1.4781
TZ2P CISD	1.8478	1.5009	1.6453	1.5076
TZ2P+diff CISD	1.8479	1.5012	1.6458	1.5078
TZ3P CISD	1.8404	1.4981	1.6414	1.5040
TZ2P(f) CISD	1.8340	1.4982	1.6401	1.5046
TZ2P(f)+diff CISD	1.8342	1.4987	1.6404	1.5051
TZ3P(2f) CISD	1.8287	1.4942	1.6381	1.4998
cc-pVTZ CISD	1.8361	1.5014	1.6446	1.5076
cc-pVQZ CISD	1.8265	1.4951	1.6378	1.5008
TZ2P EOM-CCSD[b]	(1.8650)	(1.5138)	1.6634	1.5211
TZ2P+diff EOM-CCSD	(1.8653)	(1.5141)	1.6641	1.5214
TZ3P EOM-CCSD	(1.8567)	(1.5107)	1.6587	1.5171
TZ2P(f) EOM-CCSD	(1.8493)	(1.5110)	1.6570	1.5180
TZ2P(f)+diff EOM-CCSD	(1.8498)	(1.5116)	1.6575	1.5185
TZ3P(2f) EOM-CCSD	(1.8441)	(1.5066)	1.6548	1.5128
cc-pVTZ EOM-CCSD	(1.8511)	(1.5140)	1.6616	1.5208
TZ2P CCSD	1.8650	1.5138	1.6605	1.5214
TZ2P+diff CCSD	1.8653	1.5141	1.6612	1.5217
TZ3P CCSD	1.8567	1.5107	1.6563	1.5174
TZ2P(f) CCSD	1.8493	1.5110	1.6545	1.5182
TZ2P(f)+diff CCSD	1.8498	1.5116	1.6550	1.5188
TZ3P(2f) CCSD	1.8441	1.5066	1.6526	1.5130
cc-pVTZ CCSD	1.8511	1.5140	1.6591	1.5210
cc-pVQZ CCSD	1.8418	1.5074	1.6521	1.5138
TZ2P CCSD(T)	1.8731	1.5270	1.6702	1.5335
TZ2P+diff CCSD(T)	1.8736	1.5274	1.6709	1.5339
TZ3P CCSD(T)	1.8655	1.5239	1.6658	1.5295
TZ2P(f) CCSD(T)	1.8582	1.5243	1.6639	1.5303
TZ2P(f)+diff CCSD(T)	1.8589	1.5248	1.6644	1.5309
TZ3P(2f) CCSD(T)	1.8538	1.5196	1.6620	1.5249
cc-pVTZ CCSD(T)	1.8602	1.5270	1.6687	1.5329
cc-pVQZ CCSD(T)	1.8517	1.5205	1.6616	1.5258

[a] Bond lengths are in Å. [b] EOM-CCSD is equivalent to CCSD for the ground state. Bond lengths labeled EOM-CCSD were calculated with the ACES II package.[49]

contraction[29] of Huzinaga's primitive Gaussian set[30] and are designated (10s6p/5s3p). The TZ basis set for Si is derived from McLean and Chandler's contraction[31] of Huzinaga's primitive Gaussian set[32] and is designated (12s9p/6s5p). The orbital exponents of the polarization functions are α_d(C) = 1.50 and 0.375, α_d(O) = 1.70 and 0.425, and α_d(Si) = 1.00 and 0.25 for double polarization (TZ2P); and α_d(C) = 3.00, 0.75, and 0.1875, α_d(O) = 3.40, 0.85, and 0.2125, and α_d(Si) = 2.00, 0.50, and 0.125 for triple polarization (TZ3P). The orbital exponents of the higher angular momentum functions are α_f(C) = 0.80, α_f(O) = 1.40, and α_f(Si) = 0.32 for one set of higher angular momentum functions [TZ2P(f)]; and α_f(C) = 1.60 and 0.40, α_f(O) = 2.80 and 0.70, and α_f(Si) = 0.64 and 0.16 for two sets of higher angular momentum functions [TZ3P(2f)]. The orbital exponents of the diffuse functions are α_p(C) = 0.03389 and α_s(C) = 0.04812, α_p(O) = 0.05840 and α_s(O) = 0.08993, and α_p(Si) = 0.02354 and α_s(Si) = 0.02567 for one set of diffuse functions [TZ2P+diff and TZ2P(f)+diff]. Pure angular momentum d and f functions were used throughout. The largest TZ-plus basis set, TZ3P(2f), comprises 136 contracted Gaussian functions with a contraction scheme of C and O (10s6p3d2f/5s3p3d2f), and Si (12s9p3d2f/6s5p3d2f). Finally, the two correlation-consistent basis sets, cc-pVTZ and cc-pVQZ, developed by Dunning and Woon[33,34] have also been used. The cc-pVQZ basis set consists of 169 contracted Gaussian functions with a contraction scheme of C and O (12s6p3d2f1g/5s4p3d2f1g) and Si (16s11p3d2f1g/6s5p3d2f1g).

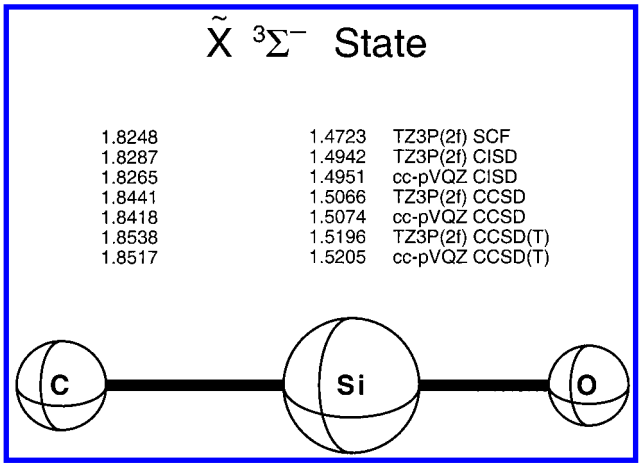

Figure 3. Predicted geometries for the $\tilde{X}\ ^3\Sigma^-$ state of CSiO at the four levels of sophistication with the TZ3P(2f) and cc-pVQZ basis sets. Bond lengths are in Å.

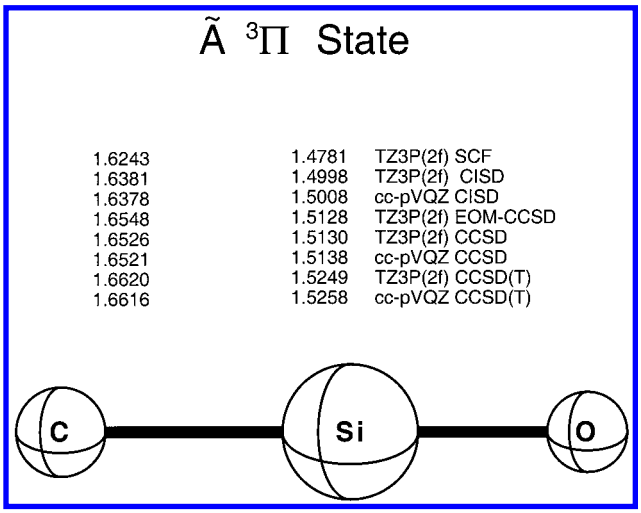

Figure 4. Predicted geometries for the $\tilde{A}\ ^3\Pi$ state of CSiO at the five levels of sophistication with the TZ3P(2f) and cc-pVQZ basis sets. Bond lengths are in Å.

The zeroth-order descriptions for the $\tilde{X}\ ^3\Sigma^-$ and $\tilde{A}\ ^3\Pi$ states of CSiO were obtained using one-configuration SCF (restricted Hartree−Fock) wave functions. Correlation effects were included using the configuration interaction with single and double excitations (CISD), coupled-cluster with single and double excitations (CCSD),[35,36] and CCSD with perturbative triple excitations [CCSD(T)][37,38] levels of theory. The $\tilde{A}\ ^3\Pi$ state of CSiO was also investigated employing the equation-of-motion (EOM) CCSD technique.[39−42] In correlated procedures with the TZ-plus basis sets, the seven core (for Si, 1s-, 2s-, and 2p-like and for C and O, 1s-like) orbitals were frozen, and the three highest-lying virtual (for Si, C, and O, 1s*-like) orbitals were deleted. The correlated wave functions with the two correlation-consistent basis sets were constructed by freezing the seven core orbitals only. With the cc-pVQZ basis set, the numbers of configuration state functions (CSFs) in the Hartree−Fock interacting spaces[43,44] in the CISD procedures are 190 782 for the $\tilde{X}\ ^3\Sigma^-$ state in C_{2v} symmetry and 375 642 in C_s symmetry, and 190 586 for the $\tilde{A}\ ^3\Pi$ state in C_{2v} symmetry and 375 151 in C_s symmetry.

The structures of the two stationary points were optimized

TABLE 2: Theoretical Predictions of the Total Energy, Dipole Moment, Harmonic Vibrational Frequencies, Infrared (IR) Intensities, and Zero-Point Vibrational Energy (ZPVE) for the $\tilde{X}\ ^3\Sigma^-$ State of the CSiO Molecule

level of theory	energy	μ_e	$\omega_1(\sigma)$ SiO stretch	$\omega_2(\pi)$ bend	$\omega_3(\sigma)$ CSi stretch	ZPVE
TZ2P SCF	−401.535 164	0.588	1416 (101.4)	181 (158.4)	624 (15.7)	3.43
TZ2P+diff SCF	−401.536 097	0.647	1415 (105.1)	179 (159.0)	626 (16.4)	3.43
TZ3P SCF	−401.537 464	0.613	1424 (100.1)	181 (156.3)	628 (16.7)	3.45
TZ2P(f) SCF	−401.539 443	0.572	1418 (101.3)	175 (166.8)	630 (14.8)	3.43
TZ2P(f)+diff SCF	−401.540 262	0.638	1416 (106.0)	169 (164.2)	631 (15.6)	3.41
TZ3P(2f) SCF	−401.544 044	0.614	1429 (100.2)	180 (158.7)	638 (16.2)	3.47
TZ2P CISD	−401.907 303	0.700	1325 (59.0)	124 (106.7)	649 (11.6)	3.18
TZ2P+diff CISD	−401.908 815	0.769	1324 (62.1)	117 (106.9)	649 (12.5)	3.15
TZ3P CISD	−401.914 388	0.713	1339 (57.8)	125 (106.8)	661 (13.2)	3.22
TZ2P(f) CISD	−401.941 625	0.646	1337 (60.6)	124 (118.6)	678 (10.8)	3.24
TZ2P(f)+diff CISD	−401.942 983	0.721	1336 (64.0)	115 (116.5)	678 (11.8)	3.21
TZ3P(2f) CISD	−401.956 798	0.673	1354 (60.2)	140 (115.2)	690 (12.4)	3.32
cc-pVTZ CISD	−401.946 499	0.577	1348 (54.5)	141 (109.9)	682 (11.0)	3.30
cc-pVQZ CISD	−401.984 627	-	1357 (−)	140 (−)	696 (−)	3.34
TZ2P CCSD	−401.954 087		1270	64	622	2.89
TZ2P+diff CCSD	−401.955 754		1269	46	622	2.83
TZ3P CCSD	−401.961 724		1285	66	634	2.93
TZ2P(f) CCSD	−401.992 060		1283	61	653	2.94
TZ2P(f)+diff CCSD	−401.993 572		1281	41	652	2.88
TZ3P(2f) CCSD	−402.008 372		1301	89	664	3.06
cc-pVTZ CCSD	−401.997 573		1294	92	657	3.05
cc-pVQZ CCSD	−402.038 281		1303	90	671	3.08
TZ2P CCSD(T)	−401.978 076		1214	31*i*	627	2.63
TZ2P+diff CCSD(T)	−401.979 858		1213	56*i*	626	2.63
TZ3P CCSD(T)	−401.986 406		1229	39*i*	636	2.67
TZ2P(f) CCSD(T)	−402.018 311		1226	79	653	2.91
TZ2P(f)+diff CCSD(T)	−402.019 920		1225	126	651	3.04
TZ3P(2f) CCSD(T)	−402.035 826		1245	129	661	3.09
cc-pVTZ CCSD(T)	−402.024 468		1238	61	656	2.88
cc-pVQZ CCSD(T)	−402.067 432		1247	60	667	2.91

[a] Total energies are in hartree, dipole moments are in debye, harmonic vibrational frequencies are in cm^{-1}, infrared (IR) intensities (in parentheses) are in km mol^{-1}, and zero-point vibrational energies (ZPVE) are in kcal/mol. IR intensities of the ω_2 mode were doubled.

using analytic derivative methods.[45−47] Harmonic vibrational frequencies at the SCF level were evaluated analytically, at the CISD level of theory by finite differences of analytic gradients, and at the CCSD, EOM-CCSD, and CCSD(T) levels of theory by five-point numerical differentiation of total energies. All computations were carried out using the PSI 2.0.8 program package,[48] except for EOM-CCSD wave functions, which were carried out using the ACES II package,[49] on IBM RS/6000 workstations.

V. Results and Discussion

The bond lengths for the ground ($\tilde{X}\ ^3\Sigma^-$) and first excited triplet ($\tilde{A}\ ^3\Pi$) states of CSiO are provided in Table 1. Figures 3 and 4 depict the optimized geometries at the four (five) levels of sophistication using the TZ3P(2f) and cc-pVQZ basis sets. The total energies and physical properties for the $\tilde{X}\ ^3\Sigma^-$ and $\tilde{A}\ ^3\Pi$ states of CSiO radical are presented in Tables 2 and 3, respectively.

A. Geometries. The optimized geometries for the $\tilde{X}\ ^3\Sigma^-$ state and $\tilde{A}\ ^3\Pi$ state of CSiO are presented in Table 1 and in Figures 3 and 4, respectively. The ground and first excited triplet states of CSiO have linear equilibrium structures, as was the case for CCO[15] and SiCO.[17] The two bonds of the two states are generally elongated with improved treatments of correlation effects and are shortened with increased basis set size. The C−Si bond of the first excited triplet state is predicted to be significantly shorter (about 0.2 Å) than that of the ground state, whereas the Si−O bond is predicted to be slightly longer (about 0.005−0.008 Å). The 9s MO in eq 1 (in Figure 1) is a lone-pair (nonbonding) orbital on the C atom, and the 3π MO (in Figure 2) has strong C−Si π bonding and weak Si−O anti-π bonding character. Consequently, a single-electron excitation in eq 2 results in a distinct contraction of the C−Si bond and a marginal elongation of the Si−O bond. With the cc-pVQZ CCSD(T) method the equilibrium bond distance of the diatomic SiO ($\tilde{X}\ ^1\Sigma^+$) is $r_e = 1.5201$ Å, while the experimental value is $r_e = 1.5097$ Å.[50] It is seen that the SiO bond distance for the $\tilde{X}\ ^3\Sigma^-$ state of CSiO is close to that of the diatomic SiO. The internuclear separations of the diatomic SiC radical were experimentally found to be $r_0 = 1.721\ 87$ Å ($\tilde{X}\ ^3\Pi$) and $r_0 = 1.813\ 56$ Å ($\tilde{A}\ ^3\Sigma^-$).[51] The r_e (CSi) for the $\tilde{X}\ ^3\Sigma^-$ state of CSiO is close to the r_0 value of the $\tilde{A}\ ^3\Sigma^-$ state of the diatomic SiC. For the $\tilde{A}\ ^3\Pi$ state, the EOM-CCSD method predicts geometries similar to those from the CCSD method rather than those from the CISD method. The sums of the bond lengths for the two states are 3.3722 (1.8517 + 1.5205) Å and 3.1874 (1.6616 + 1.5258) Å, respectively, with the cc-pVQZ CCSD(T) method. It is seen that the $\tilde{A}\ ^3\Pi$ state presents a contracted structure of about 0.185 (3.372−3.187) Å (−5.5%) compared to that of the $\tilde{X}\ ^3\Sigma^-$ state. Similar geometrical trends have been observed for the $\tilde{X}\ ^3\Sigma^-$ and $\tilde{A}\ ^3\Pi$ states of the CCO[15] and SiCO[17] systems.

Our predicted C−Si bond distance of 1.662 Å for the $\tilde{A}\ ^3\Pi$ state is one of the shortest known Si−C bond distance. Only a few Si=C double-bond distances are known experimentally, including 1.702 Å for $Me_2Si{=}C(SiMe_3)(SiMe\text{-}t\text{-}Bu)$,[52] 1.692 Å for $(CH_3)_2Si{=}CH_2$,[53] and 1.704 Å for the parent $H_2Si{=}CH_2$.[54] By this criteria, the C−Si bond in the $\tilde{A}\ ^3\Pi$ state of CSiO would appear to be a strong double bond. This is consistent with an Si−C bond of formal order 2.5, due to two electrons in the 7σ bonding orbital and three electrons in the 3π bonding orbital.

TABLE 3: Theoretical Predictions of the Total Energy, Dipole Moment, Harmonic Vibrational Frequencies, and Infrared Intensities for the $\tilde{A}\ ^3\Pi$ State of the CSiO Molecule[a]

level of theory	energy	μ_e	$\omega_1(\sigma)$ SiO stretch	$\omega_2(\pi_i, {}^3A'')$ bend	$\omega_2(\pi_o, {}^3A')$ bend	$\omega_3(\sigma)$ CSi stretch
TZ2P SCF	−401.495 785	1.988	1498 (213.7)	484 (9.1)	330 (87.8)	1071 (0.0)
TZ2P+diff SCF	−401.496 477	2.047	1496 (217.0)	482 (8.4)	329 (87.3)	1070 (0.0)
TZ3P SCF	−401.498 664	2.030	1508 (207.8)	490 (9.7)	324 (83.6)	1075 (0.0)
TZ2P(f) SCF	−401.501 583	1.955	1501 (213.8)	500 (7.7)	326 (92.2)	1072 (0.0)
TZ2P(f)+diff SCF	−401.502 209	2.020	1499 (219.2)	495 (6.3)	324 (90.4)	1071 (0.0)
TZ3P(2f) SCF	−401.506 699	1.990	1510 (209.4)	508 (7.3)	325 (84.5)	1076 (0.0)
TZ2P CISD	−401.860 379	1.752	1406 (129.5)		292 (61.2)	1000 (0.0)
TZ2P+diff CISD	−401.861 644	1.818	1404 (133.3)		290 (60.8)	999 (0.0)
TZ3P CISD	−401.868 523	1.787	1424 (127.4)		289 (58.4)	1010 (0.0)
TZ2P(f) CISD	−401.897 879	1.732	1423 (133.3)		292 (66.2)	1012 (0.0)
TZ2P(f)+diff CISD	−401.898 999	1.805	1421 (137.9)		291 (64.7)	1011 (0.0)
TZ3P(2f) CISD	−401.913 847	1.765	1437 (134.0)		296 (61.1)	1020 (0.0)
cc-pVTZ CISD	−401.901 040	1.671	1431 (121.4)		297 (59.6)	1014 (0.1)
cc-pVQZ CISD	−401.941 520	-	1440 (−)		296 (−)	1022 (−)
TZ2P EOM-CCSD	−401.904 778		1342	364	286	944
TZ2P+diff EOM-CCSD	−401.906 197		1340	357	282	942
TZ3P EOM-CCSD	−401.913 466		1362	362	282	956
TZ2P(f) EOM-CCSD	−401.946 153		1361	372	288	958
TZ2P(f)+diff EOM-CCSD	−401.947 416		1358	367	285	957
TZ3P(2f) EOM-CCSD	−401.963 204		1376	377	291	967
cc-pVTZ EOM-CCSD	−401.950 083		1370	374	291	960
TZ2P CCSD	−401.905 034		1345		271	950
TZ2P+diff CCSD	−401.906 470		1343		267	948
TZ3P CCSD	−401.913 786		1365		267	961
TZ2P(f) CCSD	−401.946 285		1363		271	964
TZ2P(f)+diff CCSD	−401.947 561		1361		269	962
TZ3P(2f) CCSD	−401.963 427		1378		276	972
cc-pVTZ CCSD	−401.950 221		1372		276	965
cc-pVQZ CCSD	−401.993 223		1382		276	974
TZ2P CCSD(T)	−401.926 824		1302		254	913
TZ2P+diff CCSD(T)	−401.928 383		1300		253	912
TZ3P CCSD(T)	−401.936 307		1316		252	920
TZ2P(f) CCSD(T)	−401.970 148		1320		256	927
TZ2P(f)+diff CCSD(T)	−401.971 529		1318		254	926
TZ3P(2f) CCSD(T)	−401.988 514		1335		262	936
cc-pVTZ CCSD(T)	−401.974 855		1329		260	929
cc-pVQZ CCSD(T)	−402.020 001		1338		261	938

[a] Total energies are in hartree, dipole moments are in debye, harmonic vibrational frequencies are in cm^{-1}, and infrared (IR) intensities (in parentheses) are in km mol^{-1}.

The only shorter Si−C bond distance determined experimentally is that very recently reported for the $\tilde{A}\ ^2\Sigma^+$ excited state of SiCH by Smith et al.[55] This group found an Si−C distance of 1.612 Å for the first excited electronic state of SiCH. Smith and coworkers describe the $\tilde{A}\ ^2\Sigma^+$ state of SiCH as incorporating a Si−C triple bond. This is consistent with our characterization of the $\tilde{A}\ ^3\Pi$ state of CSiO as a system of bond order $^5/_2$.

B. Dipole Moments. The dipole moment of the ground state, $\mu_e(^+CSiO^-) = 0.67$ D with the TZ3P(2f) CISD method, is relatively small, whereas that of the first excited triplet state, $\mu_e(^+CSiO^-) = 1.77$ D with the same method, is considerably larger. The signs indicate the direction of the dipole moments. The single-electron excitation in eq 2 appears to make the CSiO molecule more polar. This feature is also seen for the SiCO system: the dipole moment for the $\tilde{A}\ ^3\Pi$ of SiCO, $\mu_e(^+SiCO^-) = 2.49$ D with TZ3P(2f) CISD method, is markedly greater than that for the $\tilde{X}\ ^3\Sigma^-$ state of SiCO, $\mu_e(^+SiCO^-) = 0.29$ D with the same method. The theoretically predicted dipole moment of the diatomic SiO ($\tilde{X}\ ^1\Sigma^+$) is $\mu_e(^+SiO^-) = 3.28$ D with the TZ3P(2f) CISD method, whereas the experimental value is $\mu_e = 3.098$ D.[50] The dipole moments for the two low-lying states of CSiO are significantly smaller than the dipole moment of the diatomic SiO ($\tilde{X}\ ^1\Sigma^+$).

C. Harmonic Vibrational Frequencies. As seen in Table 2, the SiO stretching (ω_1) and CSi stretching (ω_3) frequencies of the $\tilde{X}\ ^3\Sigma^-$ state generally decrease with improved treatment of correlation effects because of elongated bonds. This feature is consistent with Badger's rule that a shorter bond is associated with a higher vibrational frequency (or a larger stretching force constant).[56,57] The bending (ω_2) frequency generally diminishes with the level of sophistication. At the CCSD(T) level of theory, using the smaller basis sets (i.e., those without f functions), the bending frequency becomes imaginary. The ground state of CSiO is seen to be very floppy with respect to the bending motion.

For the $\tilde{A}\ ^3\Pi$ state, all three vibrational frequencies decrease with advanced treatments of correlation effects. These three harmonic vibrational frequencies are higher for the excited triplet state than those for the ground state, probably because of the contracted structure of the $\tilde{A}\ ^3\Pi$ state, as mentioned above. The EOM-CCSD technique provides harmonic vibrational frequencies that are reasonably consistent with those from the CCSD method. The in-plane bending frequency (in the $^3A''$ state) is predicted to be larger in magnitude than the out-of-plane bending frequency (in the $^3A'$ state). With the cc-pVQZ CCSD(T) method, the harmonic vibrational frequency of the diatomic SiO ($\tilde{X}\ ^1\Sigma^+$) is predicted to be 1235 cm^{-1}, whereas the experimental value is 1241.6 cm^{-1}.[50] The SiO stretching frequency (1247 cm^{-1} with the same method) for the $\tilde{X}\ ^3\Sigma^-$ state of CSiO has a magnitude similar to that for the diatomic SiO; however, the

TABLE 4: Predicted Renner Parameter (ϵ) and Harmonic Bending Vibrational Frequency (ω_2)[a] for the $\tilde{A}\ ^3\Pi$ State of CSiO, Neglecting Anharmonicity

level of theory	$\omega_2^-(^3A'')$	$\omega_2^+(^3A')$	ϵ	ω_2
TZ2P EOM-CCSD	364	286	−0.237	327
TZ2P+diff EOM-CCSD	357	282	−0.232	322
TZ3P EOM-CCSD	362	282	−0.245	324
TZ2P(f) EOM-CCSD	372	288	−0.250	333
TZ2P(f)+diff EOM-CCSD	367	285	−0.248	329
TZ3P(2f) EOM-CCSD	377	291	−0.253	337
cc-pVTZ EOM-CCSD	374	291	−0.246	335

[a] Harmonic bending vibratrional frequencies are in cm^{-1}.

TABLE 5: Excitation Energies[a] for the $\tilde{A}\ ^3\Pi$ States of CSiO

level of theory	ΔE
TZ2P SCF	24.71, 1.072, 8640
TZ2P+diff SCF	24.86, 1.078, 8700
TZ3P SCF	24.35, 1.056, 8520
TZ2P(f) SCF	23.76, 1.030, 8310
TZ2P(f)+diff SCF	23.88, 1.035, 8350
TZ3P(2f) SCF	23.43, 1.016, 8200
TZ2P CISD	29.45, 1.277, 10300
TZ2P+diff CISD	29.60, 1.284, 10350
TZ3P CISD	28.78, 1.248, 10070
TZ2P(f)CISD	27.45, 1.190, 9600
TZ2P(f)+diff CISD	27.60, 1.197, 9650
TZ3P(2f) CISD	26.95, 1.169, 9430
cc-pVTZ CISD	28.53, 1.237, 9980
cc-pVQZ CISD	27.05, 1.173, 9460
TZ2P EOM-CCSD	30.94, 1.342, 10820
TZ2P+diff EOM-CCSD	31.10, 1.349, 10880
TZ3P EOM-CCSD	30.28, 1.313, 10590
TZ2P(f) EOM-CCSD	28.81, 1.249, 10080
TZ2P(f)+diff EOM-CCSD	28.96, 1.256, 10130
TZ3P(2f) EOM-CCSD	28.34, 1.229, 9910
cc-pVTZ EOM-CCSD	29.80, 1.292, 10420
TZ2P CCSD	30.78, 1.335, 10770
TZ2P+diff CCSD	30.93, 1.341, 10820
TZ3P CCSD	30.08, 1.304, 10520
TZ2P(f) CCSD	28.72, 1.246, 10050
TZ2P(f)+diff CCSD	28.87, 1.252, 10100
TZ3P(2f) CCSD	28.20, 1.223, 9860
cc-pVTZ CCSD	29.71, 1.289, 10390
cc-pVQZ CCSD	28.27, 1.226, 9890
TZ2P CCSD(T)	32.16, 1.395, 11250
TZ2P+diff CCSD(T)	32.30, 1.401, 11300
TZ3P CCSD(T)	31.44, 1.363, 11000
TZ2P(f) CCSD(T)	30.22, 1.311, 10570
TZ2P(f)+diff CCSD(T)	30.37, 1.317, 10620
TZ3P(2f) CCSD(T)	29.69, 1.287, 10380
cc-pVTZ CCSD(T)	31.13, 1.350, 10890
cc-pVQZ CCSD(T)	29.76, 1.291, 10410

[a] Energies are in kcal mol^{-1}, eV, and cm^{-1}.

SiO stretch of the $\tilde{A}\ ^3\Pi$ state has a higher (by 96 cm^{-1}) frequency than that for diatomic SiO.

D. Infrared (IR) Intensities. The bending (ω_2) mode of the ground state shows the strongest IR intensity, followed by the SiO stretching and CSi stretching modes. However, the ground-state bending frequency is so low ($\omega_2 \sim 60$ cm^{-1}) that experimental detection might prove difficult. The Si−O stretch has substantial IR intensity, and this fundamental should be observable near 1200 cm^{-1}. For the first excited triplet state, the SiO stretching mode presents the largest intensity. The CSi stretching mode of the $\tilde{A}\ ^3\Pi$ state has a remarkably small intensity.

E. Renner−Teller Effects. In Table 4, the Renner parameter (ϵ) and harmonic bending frequency (ω_2) for the $\tilde{A}\ ^3\Pi$ state of CSiO are presented. These values were determined utilizing the equations presented in section III, neglecting anharmonicity. The out-of-plane bending motion is assigned to the upper state (ω_2^+), as the open-shell π MO is kept symmetric during the bending vibration (in the $^3A'$ state). On the other hand, the in-plane bending motion is assigned to the lower state (ω_2^-), because the open-shell π MO is kept antisymmetric during the bending vibration (in the $^3A''$ state). The sign of the Renner parameter for the $\tilde{A}\ ^3\Pi$ state of CSiO is minus (−), as was the case for the corresponding states of CCO and SiCO. At the TZ3P(2f) EOM-CCSD level of theory, the theoretically predicted ϵ and ω_2 values for the $\tilde{A}\ ^3\Pi$ state of CSiO are $\epsilon = -0.253$ and $\omega_2 = 337$ cm^{-1}. With the same method, the corresponding ϵ and ω_2 values for the $\tilde{A}\ ^3\Pi$ state of CCO[15] are $\epsilon = -0.153$ and $\omega_2 = 627$ cm^{-1}, compared to the experimental values of $\epsilon = -0.172$ and $\omega_2 = 607.8$ cm^{-1}.[5] The predicted values for the $\tilde{A}\ ^3\Pi$ state of SiCO[17] are $\epsilon = -0.103$ and $\omega_2 = 447$ cm^{-1}. Experimental values are not available for SiCO. Among the $\tilde{A}\ ^3\Pi$ states of the three ketenylidene type molecules, the CSiO radical presents the largest Renner parameter, whereas the SiCO radical has the smallest ϵ value.

TABLE 6: Bond Dissociation (C−SiO) Energies (D_e) for the $\tilde{X}\ ^3\Sigma^-$ State of CSiO

level of theory	in kcal mol^{-1}	in eV
TZ2P SCF	6.09 (4.66)	0.264 (0.202)
TZ2P+diff SCF	6.08 (4.65)	0.264 (0.202)
TZ3P SCF	6.33 (4.89)	0.274 (0.212)
TZ2P(f) SCF	6.96 (5.54)	0.302 (0.240)
TZ2P(f)+diff SCF	6.79 (5.38)	0.294 (0.233)
TZ3P(2f) SCF	7.63 (6.17)	0.331 (0.268)
TZ2P CCSD	21.27 (20.18)	0.922 (0.875)
TZ2P+diff CCSD	21.15 (20.12)	0.917 (0.872)
TZ3P CCSD	22.06 (20.95)	0.957 (0.908)
TZ2P(f) CCSD	25.66 (24.54)	1.113 (1.064)
TZ2P(f)+diff CCSD	25.47 (24.41)	1.104 (1.059)
TZ3P(2f) CCSD	27.36 (26.14)	1.186 (1.134)
cc-pVTZ CCSD	26.35 (25.13)	1.143 (1.090)
cc-pVQZ CCSD	28.09 (26.85)	1.218 (1.164)
TZ2P CCSD(T)	25.34 (24.44)	1.099 (1.060)
TZ2P+diff CCSD(T)	25.19 (24.28)	1.092 (1.053)
TZ3P CCSD(T)	26.14 (25.21)	1.134 (1.093)
TZ2P(f) CCSD(T)	29.95 (28.78)	1.299 (1.248)
TZ2P(f)+diff CCSD(T)	29.74 (28.44)	1.290 (1.233)
TZ3P(2f) CCSD(T)	31.72 (30.39)	1.376 (1.318)
cc-pVTZ CCSD(T)	30.64 (29.51)	1.329 (1.280)
cc-pVQZ CCSD(T)	32.58 (31.44)	1.413 (1.363)

[a] D_0 values are in parentheses.

F. Energetics. Table 5 contains the excitation energies for the $\tilde{A}\ ^3\Pi$ state relative to the $\tilde{X}\ ^3\Sigma^-$ state at all levels of theory employed in the present study. With the TZ3P(2f) basis set, the excitation energies for the $\tilde{A}\ ^3\Pi$ state of CSiO were predicted to be 23.4 (SCF), 27.0 (CISD), 28.3 (EOM-CCD), 28.2 (CCSD), and 29.7 kcal/mol [CCSD(T)]. Improved treatment of correlation effects generally increases this energy separation, whereas the increase of the basis set size decreases the energy difference. It should be noted that the EOM-CCSD technique presents an energy separation similar to that from the CCSD method with a given basis set. It is clearly seen that the $\tilde{X}-\tilde{A}$ splitting is converging to the most reliable value in terms of the correlation level and basis set expansion. At the highest level of theory, cc-pVQZ CCSD(T), the classical $\tilde{X}-\tilde{A}$ splitting (T_e value) was predicted to be 29.8 kcal/mol (1.29 eV, 10 400 cm^{-1}), which is smaller than the corresponding value of 33.1 kcal/mol for the isovalent CCO radical[15] and less than one-half the value of 68.5 kcal/mol for the isoelectronic SiCO radical.[17] Utilizing the three cc-pVQZ CCSD(T) harmonic vibrational frequencies for the $\tilde{X}\ ^3\Sigma^-$ state and the two cc-pVQZ CCSD(T) harmonic stretching

TABLE 7: Comparison of the Ketenylidene XYO (X, Y = C, Si) Type Radicals

physical properties	CCO[a]	SiCO[b]	CSiO[c]
Renner−Teller type[d]			
$\tilde{A}\ ^3\Pi$	A	A	A
XY distance[e]			
$\tilde{X}\ ^3\Sigma^-$	1.370	1.825	1.854
$\tilde{A}\ ^3\Pi$	1.274	1.706	1.662
	(−7.0%)	(−6.5%)	(−10.4%)
YO distance[e]			
$\tilde{X}\ ^3\Sigma^-$	1.163	1.159	1.520
$\tilde{A}\ ^3\Pi$	1.186	1.176	1.525
	(+2.0%)	(+1.5%)	(+0.3%)
XO distance[e]			
$\tilde{X}\ ^3\Sigma^-$	2.533	2.984	3.373
$\tilde{A}\ ^3\Pi$	2.460	2.882	3.187
	(−2.9%)	(−3.4%)	(−5.5%)
dipole moment[f]			
$\tilde{X}\ ^3\Sigma^-$	1.42	0.29	0.67
$\tilde{A}\ ^3\Pi$	1.47	2.49	1.77
$\tilde{X}-\tilde{A}$ splitting[g]	33.1	68.5	29.8

[a] From ref 15. [b] From ref 17. [c] From this study. [d] See text and ref 24. [e] Bond distances are in Å with the TZ3P(2f) CCSD(T) method. [f] Dipole moments are in debye with the TZ3P(2f) CISD method. [g] Splittings (T_e values) are in kcal mol^{-1} with the cc-pVQZ CCSD(T) method.

frequencies with double the TZ3P(2f) EOM-CCSD ω_2 frequency for the $\tilde{A}\ ^3\Pi$ state, the zero-point vibrational energy (ZPVE) correction between the two states becomes 458 cm^{-1}. Consequently, the quantum mechanical splitting (T_0 value) is determined to be 10 900 cm^{-1} (31.1 kcal/mol, 1.35 eV).

G. Bond Energy for C−SiO. The bond energy for C−SiO was evaluated from the dissociation reaction

$$\mathrm{CSiO}\ (\tilde{X}\ ^3\Sigma^-) \rightarrow \mathrm{C}\ (^3\mathrm{P}) + \mathrm{SiO}\ (\tilde{X}\ ^1\Sigma^+) \qquad (11)$$

In Table 6, the bond energies for C−SiO at the SCF, CCSD, and CCSD(T) levels of theory are presented. It should be noted that these three methods are size-consistent. The bond energy, dissociation energy for eq 11, is observed to be quite sensitive to correlation effects and basis set size. It is seen that the dissociation energies from the SCF method are not reliable at all. With the most reliable method, cc-pVQZ CCSD(T), the bond energy for C−SiO is predicted to be $D_e = 32.6$ kcal/mol (1.41 eV), or $D_0 = 31.4$ kcal/mol (1.36 eV), indicating that the ground state of CSiO is considerably stable, thermodynamically, against the dissociation reaction.

H. Relative Stability of CSiO and SiCO. With the TZ3P-(2f) CCSD(T) method, the total energies of the ground states of SiCO and CSiO are −402.142 373 ($\tilde{X}\ ^3\Sigma^-$ SiCO)[17] and −402.035 826 hartrees ($\tilde{X}\ ^3\Sigma^-$ CSiO) (this study). Consequently, the $\tilde{X}\ ^3\Sigma^-$ state of CSiO lies 66.9 kcal/mol above the $\tilde{X}\ ^3\Sigma^-$ state of SiCO. With the zero-point vibrational energy correction, this energy separation becomes 65.4 kcal/mol.

I. Comparisons Among CCO, SiCO, and CSiO. In Table 7, the structural characteristics and energetics are compared for the ketenylidene (CCO) and monosilaketenylidene (SiCO and CSiO) radicals. The first excited triplet states ($\tilde{A}\ ^3\Pi$) of these three radicals are classified as type A Renner−Teller molecules. The XY (X,Y = C, Si) bonds of the three molecules are contracted during the $\tilde{A} \leftarrow \tilde{X}$ excitation, whereas the YO (Y = C, Si) bonds are elongated. The percentage shortening of the molecular size (XO distance) for the $\tilde{A}\ ^3\Pi$ state relative to the ground state is in the order

$$\mathrm{CSiO} > \mathrm{SiCO} > \mathrm{CCO} \qquad (12)$$

The magnitudes of the dipole moments for the ground state of the three species are in the order

$$\mathrm{CCO} > \mathrm{CSiO} > \mathrm{SiCO} \qquad (13)$$

whereas those for the first excited triplet states are in the order

$$\mathrm{SiCO} > \mathrm{CSiO} > \mathrm{CCO} \qquad (14)$$

It is seen that CCO is the most polar for the ground state, whereas SiCO is the most polar for the first excited triplet state. The $\tilde{X}-\tilde{A}$ splitting is the largest for the SiCO radical followed by those for the CCO and CSiO radicals.

VI. Concluding Remarks

The two lowest-lying triplet states of the 2-silaketenylidene radical have been investigated employing ab initio electronic structure theory. The $\tilde{X}\ ^3\Sigma^-$ and $\tilde{A}\ ^3\Pi$ states of CSiO are found to be linear, as was the case for the isovalent CCO and isoelectronic SiCO radicals. The $\tilde{A}\ ^3\Pi$ state of CSiO is classified as a type A Renner−Teller molecule, and its Renner parameter and harmonic bending frequency are determined to be $\epsilon = -0.253$ and $\omega_2 = 337$ cm^{-1}. With our most reliable level of theory, cc-pVQZ CCSD(T), the classical $\tilde{X}-\tilde{A}$ splitting of CSiO has been predicted to be 29.8 kcal/mol (1.29 eV, 10 400 cm^{-1}), and the quantum mechanical energy separation to be 31.1 kcal/mol (1.35 eV, 10 900 cm^{-1}). With the same method, the bond energy for the ground state of the CSiO radical was determined to be $D_e = 32.6$ ($D_0 = 31.4$) kcal/mol, which indicates that CSiO is thermodynamically stable in its ground state.

Acknowledgment. This research was supported by the U. S. National Science Foundation, Grant CHE-9815397.

References and Notes

(1) Pitts, W. M.; Donnelly, V. M.; Baronavski, A. P.; McDonald, J. R. *Chem. Phys.* **1981**, *61*, 451.
(2) Ohashi, M.; Suzuki, H.; Ishikawa, S.; Yamada, C.; Kanamori, H.; Irvine, W. M.; Brown, R. D.; Godfrey, P. D.; Kaifu, N. *Astophys. J.* **1991**, *380*, L39.
(3) Jacox, M. E.; Milligan, D. E.; Moll, N. G.; Thompson, W. E. *J. Chem. Phys.* **1965**, *43*, 3734.
(4) Devillers, M. C. *C. R. Acad. Sci.* **1966**, *262c*, 1485.
(5) Devillers, M. C.; Ramsay, D. A. *Can. J. Phys.* **1971**, *49*, 2839.
(6) Lembke, R. R.; Ferrante, R. F.; Weltner, W. *J. Am. Chem. Soc.* **1977**, *99*, 416.
(7) Jacox, M. E. Vibrational and Electronic Energy Levels of Polyatomic Transient Molecules. *Journal of Physical and Chemical Reference Data*; American Institute of Physics: Woodbury, NY, 1994; Monograph No. 3.
(8) Walch, S. P. *J. Chem. Phys.* **1980**, *72*, 5679.
(9) Chabalowski, C.; Buenker, R. J.; Peyerimoff, S. D. *J. Chem. Phys.* **1986**, *84*, 268.
(10) DeKock, R. L.; Grev, R. S.; Schaefer, H. F. *J. Chem. Phys.* **1988**, *89*, 3016.
(11) Maclagan, R. G. A. R.; Sudkeaw, P. *J. Chem. Soc., Faraday Trans.* **1993**, *89*, 3325.
(12) Suter, H. U.; Huang, M.-B.; Engels, B. *J. Chem. Phys.* **1994**, *101*, 7686.
(13) Zengin, V.; Persson, B. J.; Strong, K. M.; Continetti, R. E. *J. Chem. Phys.* **1996**, *105*, 9740.
(14) Choi, H.; Mordaunt, D. H.; Bise, R. T.; Taylor, T. R.; Neumark, D. M. *J. Chem. Phys.* **1996**, *108*, 4070.
(15) Brown, S. T.; Yamaguchi, Y.; Schaefer, H. F. *J. Phys. Chem.*, in press.
(16) Cai, Z.-L.; Wang, Y.-F.; Xiao, H.-M. *Chem. Phys. Lett.* **1992**, *191*, 533.
(17) Petraco, N. D. K.; Brown, S. T.; Yamaguchi, Y.; Schaefer, H. F. *J. Chem. Phys.* **2000**, *112*, 3201.
(18) Herzberg, G.; Teller, E. *Z. Phys. Chem. Abt. B* **1933**, *21*, 410.
(19) Renner, R. *Z. Phys.* **1934**, *92*, 172.
(20) Hougen, J. T. *J. Chem. Phys.* **1961**, *36*, 1874.

(21) Herzberg, H. *Molecular Spectra and Molecular Structure III. Electronic Spectra and Electronic Structure of Polyatomic Molecules*; Van Nostrand: Princeton, NJ, 1966.
(22) Jungen, Ch.; Merer, A. J. In *Molecular Spectroscopy: Modern Research*; Rao, K. N., Ed.; Academic: New York, 1976; Vol. 2, p 127.
(23) Brown J. M.; Jørgensen, F. *Adv. Chem. Phys.* **1983**, *52*, 117.
(24) Lee, T. J.; Fox, D. J.; Schaefer, H. F.; Pitzer, R. M. *J. Chem. Phys.* **1984**, *81*, 356.
(25) Bunker, P. R.; Jensen, P. *Molecular Symmetry and Spectroscopy*, 2nd ed.; NRC Research Press: Ottawa, Canada, 1998.
(26) Yamaguchi, Y.; Alberts, I. L.; Goddard, J. D.; Schaefer, H. F. *Chem. Phys.* **1990**, *147*, 309.
(27) Burton, N. A.; Yamaguchi, Y.; Alberts, I. L.; Schaefer, H. F. *J. Chem. Phys.* **1991**, *95*, 7466.
(28) Crawford, T. D.; Stanton, J. F.; Allen, W. D.; Schaefer, H. F. *J. Chem. Phys.* **1990**, *107*, 10626.
(29) Dunning, T. H. *J. Chem. Phys.* **1972**, *55*, 716.
(30) Huzinaga, S. *J. Chem. Phys.* **1965**, *42*, 1293.
(31) McLean, A. D.; Chandler, G. S. *J. Chem. Phys.* **1980**, *72*, 5639.
(32) Huzinaga, S. *Approximate Atomic Functions II*; Department of Chemistry Report; University of Alberta: Edmonton, Alberta, Canada, 1971.
(33) Dunning, T. H. *J. Chem. Phys.* **1989**, *90*, 1007.
(34) Woon, D. E.; Dunning, T. H. *J. Chem. Phys.* **1993**, *98*, 1358.
(35) Purvis, G. D.; Bartlett, R. J. *J. Chem. Phys.* **1982**, *76*, 1910.
(36) Rittby, M.; Bartlett, R. J. *J. Phys. Chem.* **1988**, *92*, 3033.
(37) Raghavachari, K.; Trucks, G. W.; Pople, J. A.; Head-Gorden, M. *Chem. Phys. Lett.* **1989**, *157*, 479.
(38) Scuseria, G. E. *Chem. Phys. Lett.* **1991**, *176*, 27.
(39) Monkhorst, H. J. *Int. J. Quantum Chem.* **1977**, *S11*, 421.
(40) Bartlett, R. J. In *Modern Electronic Structure Theory*; Yarkony, D. R., Ed.; World Scientific: Singapore, 1995.
(41) Stanton, J. F.; Bartlett, R. J. *J. Chem. Phys.* **1993**, *98*, 7029.
(42) Comeau, D. C.; Bartlett, R. J. *Chem. Phys. Lett.* **1993**, *207*, 414.
(43) Bunge, A. *J. Chem. Phys.* **1970**, *53*, 20.
(44) Bender, C. F.; Schaefer, H. F. *J. Chem. Phys.* **1971**, *55*, 4789.
(45) Pulay, P. *Mol. Phys.* **1969**, *17*, 197.
(46) Pulay, P. In *Modern Theoretical Chemistry*; Schaefer, H. F., Ed.; Plenum Press: New York, 1977.
(47) Yamaguchi, Y.; Osamura, Y.; Goddard, J. D.; Schaefer, H. F. *A New Dimension to Quantum Chemistry: Analytic Derivative Methods in Ab Initio Molecular Electronic Structure Theory*; Oxford University Press: New York, 1994.
(48) Janssen, C. L.; Seidl, E. T.; Scuseria, G. E.; Hamilton, T. P.; Yamaguchi, Y.; Remington, R. B.; Xie, Y.; Vacek, G.; Sherrill, C. D.; Crawford, T. D.; Fermann, J. T.; Allen, W. D.; Brooks, B. R.; Fitzgerald, G. B.; Fox, D. J.; Gaw, J. F.; Handy, N. C.; Laidig, W. D.; Lee, T. J.; Pitzer, R. M.; Rice, J. E.; Saxe, P.; Scheiner, A. C.; Schaefer, H. F. PSI 2.0.8; PSITECH, Inc.: Watkinsville, GA, 1994.
(49) Stanton, J. F.; Gauss, J.; Watts, J. D.; Nooijen, M.; Oliphant, N.; Perera, S. A.; Szalay, P. G.; Lauderdale, W. J.; Kucharski, S.A.; Gwaltney, S. R.; Beck, S.; Balková, A.; Bernholdt, D. E.; Baeck, K. K.; Rozyczko, P.; Sekino, H.; Hober, C.; Bartlett, R. J. *ACES II*; Quantum Theory Project, University of Florida: Gainsville, FL. The package also contains modified versions of the MOLECULE Gaussian integral program of Almlöf, J., Taylor, P. R.; the ABACUS integral derivative program written by Helgaker, T. U., Jensen, H. J. Aa., Jørgensen, P., Taylor, P. R.; and the PROPS property evaluation integral code of Taylor, P. R.
(50) Huber, K. P.; Herzberg, G. *Constants of Diatomic Molecules*; Van Nostrand Reinhold: New York, 1979.
(51) Brazier, C. R.; O'Brien, L. C.; Bernath, P. F. *J. Chem. Phys.* **1989**, *91*, 7384.
(52) Wiberg, N.; Wagner, G.; Riede, J.; Müller, G. *Organometallics* **1987**, *6*, 32.
(53) Gutowsky, H. S.; Chen, J.; Hajduk, P. J.; Keen, J. D.; Chuang, C.; Emilsson, T. *J. Am. Chem. Soc.* **1991**, *113*, 4747.
(54) Bailleux, S.; Bogey, M.; Demaison, J.; Bürger, H.; Senzlober, M.; Breidung, J.; Thiel, W.; Fajgar, R.; Pola, J. *J. Chem. Phys.* **1997**, *106*, 10016.
(55) Smith, T. C.; Li, H.; Clouthier, D. J.; Kingston, C. T.; Merer, A. J. *J. Chem. Phys.* **2000**, *112*, 3662.
(56) Badger, R. M. *J. Chem. Phys.* **1934**, *2*, 128.
(57) Badger, R. M. *J. Chem. Phys.* **1935**, *3*, 710.